Validity of the two-term Boltzmann approximation employed in the fluid model for high-power microwave breakdown in gas*

Zhao Peng-Cheng(赵朋程), Liao Cheng(廖 成)†, Yang Dan(杨 丹), and Zhong Xuan-Ming(钟选明)

Institute of Electromagnetics, Southwest Jiaotong University, Chengdu 610031, *China*

(Received 4 June 2013; revised manuscript received 7 September 2013; published online 25 March 2014)

The electron energy distribution function (EEDF), predicted by the Boltzmann equation solver BOLSIG+ based on the two-term approximation, is introduced into the fluid model for simulating the high-power microwave (HPM) breakdown in argon, nitrogen, and air, and its validity is examined by comparing with the results of particle-in-cell Monte Carlo collision (PIC/MCC) simulations as well as the experimental data. Numerical results show that, the breakdown time of the fluid model with the Maxwellian EEDF matches that of the PIC/MCC simulations in nitrogen; however, in argon under high pressures, the results from the Maxwellian EEDF were poor. This is due to an overestimation of the energy tail of the Maxwellian EEDF in argon breakdown. The prediction of the fluid model with the BOLSIG+ EEDF, however, agrees very well with the PIC/MCC prediction in nitrogen and argon over a wide range of pressures. The accuracy of the fluid model with the BOLSIG+ EEDF is also verified by the experimental results of the air breakdown.

Keywords: fluid model, electron energy distribution function, gas breakdown, particle-in-cell Monte Carlo collision (PIC/MCC) simulation

PACS: 51.50.+v, 52.80.Pi, 52.35.Mw **DOI:** 10.1088/1674-1056/23/5/055101

1. Introduction

The high-power microwave (HPM) has important applications in many fields, such as earth–space communications, directed energy weapons, and the creation of artificial ionized layers. The multi-giga-watt HPM technologies have been developed successfully.[1–3] When the field strength of the HPM is higher than the gas breakdown threshold, a space–time dependent plasma produced by the ionization of gas will strongly affect the wave propagation. In other words, the gas breakdown has become one of the major facts limiting the HPM transmission and radiation.

A lot of theoretical and experimental researches have been carried out to study the gas breakdown.[4–7] However, there are still many unresolved issues, such as the source of the first electron.[8] Because of its simplicity and speed, the fluid model has been widely used in the simulation of the gas breakdown by the HPM.[9,10] In the fluid model, the electron energy distribution function (EEDF), which is an important parameter to calculate the transport coefficients (ionization frequency, collision frequency, and electron energy loss frequency), is often assumed to be a Maxwellian one. However, this assumption could lead to poor predictions of the gas breakdown if the EEDF deviates noticeably from the equilibrium.[11,12] A fast method for finding the EEDF is to solve the electron Boltzmann equation (BE) directly. Based on the classic two-term approximation, a user-friendly BE solver BOLSIG+ has been developed by Hagelaar and Pitchford.[13] However, we know very little about the validity of the EEDF from BOLSIG+ for the HPM breakdown in gas.

In this paper, we use argon, nitrogen, and air as test gases. The BOLSIG+ EEDF and the Maxwellian EEDF are introduced into the fluid model respectively, and the argon, nitrogen, and air breakdowns driven by the HPM are simulated numerically. In order to validate the BOLSIG+ EEDF, the breakdown predictions of the fluid model with these two EEDFs are compared with the results of particle-in-cell Monte Carlo collision (PIC/MCC) simulations as well as the experimental data. Here the one-dimensional PIC/MCC model,[14–16] which is one of the most accurate simulation tools for the study of plasma physics, is employed to predict the EEDF and the breakdown time, and simulate the time evolution of the breakdown.

2. Model and method

The basic equations in the one-dimensional fluid model[17] are as follows:

$$\frac{\partial E_x}{\partial t} = -\left(\frac{1}{\varepsilon_0}\right)\frac{\partial H_y}{\partial z} - \frac{q_e U_x}{\varepsilon_0}, \tag{1}$$

$$\frac{\partial E_z}{\partial t} = -\frac{q_e U_z}{\varepsilon_0}, \tag{2}$$

$$\frac{\partial H_y}{\partial t} = -\left(\frac{1}{\mu_0}\right)\frac{\partial E_x}{\partial z}, \tag{3}$$

$$\frac{\partial N_e}{\partial t} = \nu_i N_e - \frac{\partial (N_e u_z)}{\partial z}, \tag{4}$$

$$\frac{\partial U_x}{\partial t} = \frac{q_e}{m_e} N_e E_x - \frac{q_e}{m_e}\mu_0 U_z H_y - \nu_c U_x, \tag{5}$$

*Project supported by the National Basic Research Program of China (Grant No. 2013CB328904), the Fundamental Research Funds for the Central Universities, China, and the Open Research Fund of Key Laboratory of Cognitive Radio and Information Processing of Ministry of Education of China.

†Corresponding author. E-mail: c.liao@swjtu.edu.cn

© 2014 Chinese Physical Society and IOP Publishing Ltd

$$\frac{\partial U_z}{\partial t} = \frac{q_e}{m_e} N_e E_z + \frac{q_e}{m_e} \mu_0 U_x H_y - \nu_c U_z - m_e \frac{\partial U_e}{\partial z}, \quad (6)$$

$$\frac{\partial U_e}{\partial t} = q_e (U_x E_x + U_z E_z) - \frac{\partial \bar{v}_z}{\partial z} U_e - N_e \nu_l, \quad (7)$$

where E_x and E_z represent the electric field components along the x axis and the z axis, respectively, H_y is the magnetic component along the y axis, q_e and m_e denote the charge and the mass of an electron, respectively, and ε_0 and μ_0 are the permittivity and the permeability of free space, respectively. The transport coefficients ν_i, ν_c, and ν_l are the ionization, collision, and energy loss frequencies, respectively, N_e denotes the free electron density, U_x and U_z are the components of the electron fluid velocity along the x axis and the z axis, and U_e is the energy of the electron fluid. The U_x, U_z, and U_e can be written as

$$U_x = N_e \bar{v}_x, \quad U_z = N_e \bar{v}_z, \quad U_e = N_e \bar{\varepsilon}_e, \quad (8)$$

where $\bar{v}_x$ and $\bar{v}_z$ denote the mean electron velocities of the electron fluid along the x axis and the z axis, respectively, and $\bar{\varepsilon}_e$ denotes the mean electron energy.

The transport coefficients are important to describe the interaction of neutral molecules and the electrons accelerated by the HPM, as shown in Eqs. (4)–(7). These coefficients can be obtained as follows:

$$\nu_i = N_{gas} \int_0^\infty \sqrt{\frac{2\varepsilon_e}{m_e}} \sigma_i f(\varepsilon_e) \mathrm{d}\varepsilon_e, \quad (9)$$

$$\nu_c = N_{gas} \int_0^\infty \sqrt{\frac{2\varepsilon_e}{m_e}} \sigma_c f(\varepsilon_e) \mathrm{d}\varepsilon_e, \quad (10)$$

$$\nu_l = N_{gas} \left[\frac{8}{3\sqrt{\pi}} \frac{m_e}{M_{gas}} \int_0^\infty \sqrt{\frac{2\varepsilon_e}{m_e}} \sigma_c f(\varepsilon_e) \varepsilon_e \mathrm{d}\varepsilon_e + \sum_{n, n \neq c} \int_0^\infty \sqrt{\frac{2\varepsilon_e}{m_e}} \sigma_n f(\varepsilon_e) \varepsilon_n \mathrm{d}\varepsilon_e \right], \quad (11)$$

where M_{gas} and N_{gas} are the mass and the density of the gas molecule (atom), respectively, σ_i and σ_c are the ionization cross section and the momentum transfer cross section, respectively, σ_n is the inelastic collision cross section, and ε_n is the threshold energy of the inelastic collision reaction. These cross sections and threshold energies for argon, nitrogen, and air can be found in Ref. [18]. The $f(\varepsilon_e)$ is the normalized EEDF.

The electron BE for a non-equilibrium assemble in an ionized gas is

$$\frac{\partial F}{\partial t} + \boldsymbol{v} \cdot \nabla F - \frac{q_e}{m_e} \boldsymbol{E} \cdot \nabla_{\boldsymbol{v}} F = C[F], \quad (12)$$

where F is the electron distribution in the six-dimensional phase space, and C represents the rate of change in F due to the collisions. Using the classic two-term approximation, the BE solver BOLSIG+ is developed by Hagelaar and Pitchford,[13] which is able to account for different growth models, quasi-stationary and oscillating fields, electron–neutral collisions, and so on. Hence, the EEDF $f(\varepsilon_e)$ in Eqs. (9)–(11) can be obtained by making use of BOLSIG+, and its accuracy will be verified in the following section.

The finite-difference time-domain (FDTD) method has been employed to solve numerically the fluid model above.[19] In our FDTD scheme, H_y, U_x, and U_z are at the half nodes, and E_x, E_z, N_e, and U_e are at the integer grid nodes. At the same time, the mean electron energies at the nodes are calculated by $\bar{\varepsilon}_e = U_e / N_e$. By substituting the corresponding $\bar{\varepsilon}_e$ into Eqs. (9)–(11), the transport coefficients can be updated at each time step. At the initial time, we assume that there is a small number of seed electrons ($N_{e0} = 1.0\ \mathrm{cm}^{-3}$) in the gas.

3. Results and discussion

Figure 1 shows the comparisons among the normalized EEDF for argon from the PIC/MCC simulations, the Maxwellian EEDF, and the EEDF from the BE solver BOLSIG+ at $E_m = 2.82$ MV/m and $f = 2.85$ GHz, where E_m and f represent the amplitude and the frequency of the HPM, respectively, and p is the gas pressure. We can see from Figs. 1(a) and 1(b) that, at high pressures (e.g., 500 Torr and 200 Torr), the energy tail of the Maxwellian EEDF is overestimated compared to that of the PIC/MCC EEDF. As the pressure decreases (e.g., 50 Torr), the collision frequency decreases, so the electrons can obtain higher energy and the EEDF is extended to the high energy region, as shown in Fig. 1(c). It can also be seen from this figure that the Maxwellian EEDF is similar to the PIC/MCC EEDF at low pressures. The BOLSIG+ EEDF, however, approximates well the PIC/MCC EEDF over all pressures.

The energy tail of the EEDF is most important in the breakdown process since it determines the ionization frequency, as shown in Fig. 2(a). In Fig. 2, the ionization, collision, and energy loss frequencies normalized to the gas density (ν / N_{gas}) for argon from the Maxwellian EEDF and the BOLSIG+ EEDF are shown as functions of the mean electron energy. It should be pointed out that, under a given electric field, the mean electron energy is low at high pressures, while high at low pressures. For example, when the electric field amplitude $E_m = 2.82$ MV/m, the time average of the mean electron energy at $p = 500$ Torr, 200 Torr, and 50 Torr is 7.2 eV, 8.8 eV, and 17.6 eV, respectively, and the corresponding EEDF is shown in Fig. 1. Figure 2(a) shows that the Maxwellian EEDF leads to a higher reduced ionization frequency (ν_i / N_{gas}) than the BOLSIG+ EEDF does when the mean electron energy is below 10 eV. This is due to the overestimation of the energy tail of the Maxwellian EEDF, as shown in Figs. 1(a) and 1(b). However, above 10 eV, since the difference between the Maxwellian EEDF and the BOLSIG+ EEDF is very small

(Fig. 1(c)), the corresponding reduced ionization frequencies are approximately equal. It can be seen from Fig. 2(b) that the reduced collision frequency ν_c/N_{gas} is weakly dependent on the shape of the EEDF. From Fig. 2(c), we can see that the reduced energy loss frequency ν_l/N_{gas} from the Maxwellian EEDF is much higher than that based on the BOLSIG+ EEDF below 10 eV, but above 10 eV, the difference of the reduced energy loss frequencies from the Maxwellian EEDF and the BOLSIG+ EEDF is not obvious. The results also indicate that, only at high mean electron energies (corresponding to low-pressure cases in general), the reduced transport coefficients based on the Maxwellian EEDF are valid for the argon breakdown by the HPM.

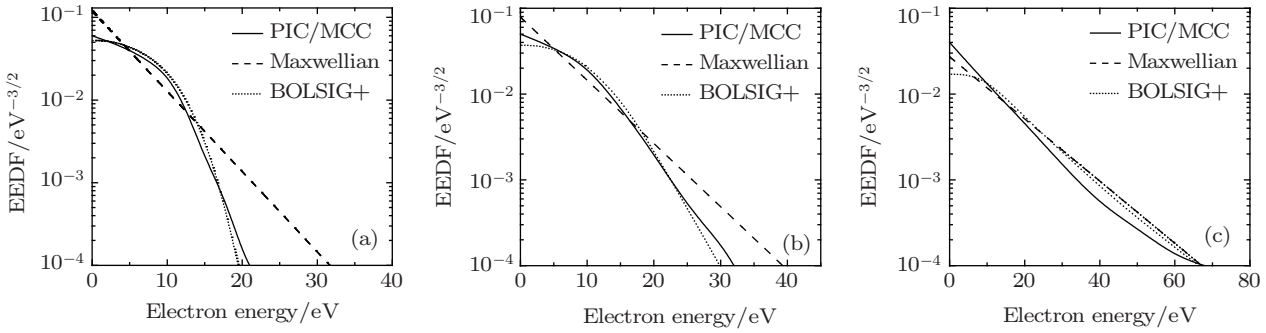


Fig. 1. The PIC/MCC EEDF, the Maxwellian EEDF, and the BOLSIG+ EEDF at $E_m = 2.82$ MV/m and $f = 2.85$ GHz: (a) $p =$ 500 Torr, (b) $p = 200$ Torr, (c) $p = 50$ Torr.

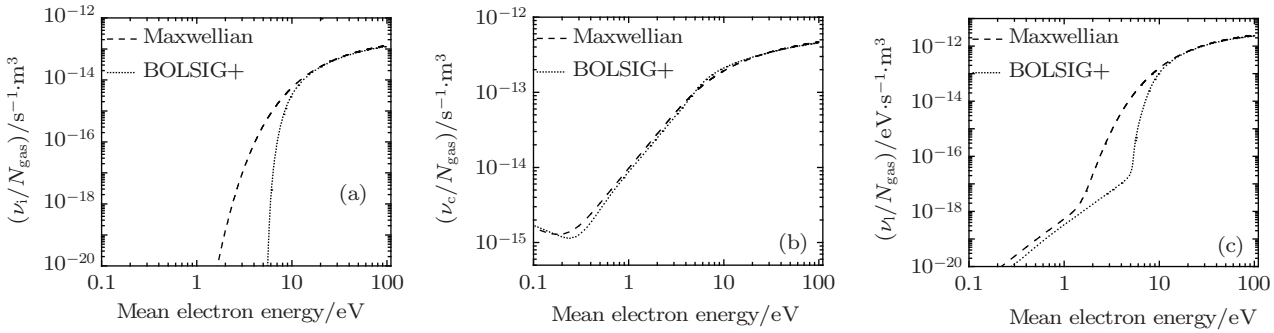


Fig. 2. The reduced transport coefficients ν/N_{gas} from the Maxwellian EEDF and the BOLSIG+ EEDF: (a) reduced ionization frequency ν_i/N_{gas}, (b) reduced collision frequency ν_c/N_{gas}, (c) reduced energy loss frequency ν_l/N_{gas}.

Before discussing the effects of different EEDFs on the argon breakdown, we first briefly introduce the time evolution of the gas (e.g., argon) breakdown under different pressures using the PIC/MCC simulations, as shown in Figs. 3–5. The amplitude and the frequency of the incident field are 2.82 MV/m and 2.85 GHz, respectively. Under high pressures, electrons suffer lots of collisions and lose a significant amount of energy gained from the microwave field. Therefore, the mean electron energy is low and the electron density grows slowly due to the low ionization frequency, as shown in Fig. 3. As the pressure decreases, the collision frequency decreases, the mean electron energy increases and the electron density grows rapidly, as shown in Figs. 4 and 5. The detailed physic mechanisms for the microwave breakdown in gas can refer to Refs. [10] and [16].

The effects of different EEDFs on the time evolution of the argon breakdown are shown in Figs. 3–5. Since the high energy tail of the Maxwellian EEDF results in an overestimation of the energy loss frequency below 10 eV (Fig. 2(c)), the mean electron energy of the fluid model with the Maxwellian EEDF under high pressures (e.g., 500 Torr and 200 Torr) is much lower than that from the PIC/MCC simulations, as shown in Figs. 3(a) and 4(a). However, we can see from Figs. 3(b) and 4(b) that the electron density from the Maxwellian EEDF grows more quickly than that from the PIC/MCC simulations. This is because the ionization frequency based on the Maxwellian EEDF is higher (Fig. 4(a)). The time evolution from the fluid model with the BOLSIG+ EEDF, however, agrees very well with that in the PIC/MCC simulations under high pressures. Under low pressures (e.g., 50 Torr), the mean electron energy is higher than 10 eV, as shown in Fig. 5. In this case, the Maxwellian and

the BOLSIG+ EEDFs approximate well the PIC/MCC EEDF (Fig. 1(c)), and the corresponding transport coefficients are approximately equal (Fig. 2). Therefore, the time evolution from the fluid model with the Maxwellian EEDF or with the BOLSIG+ EEDF is similar to that in the PIC/MCC simulations.

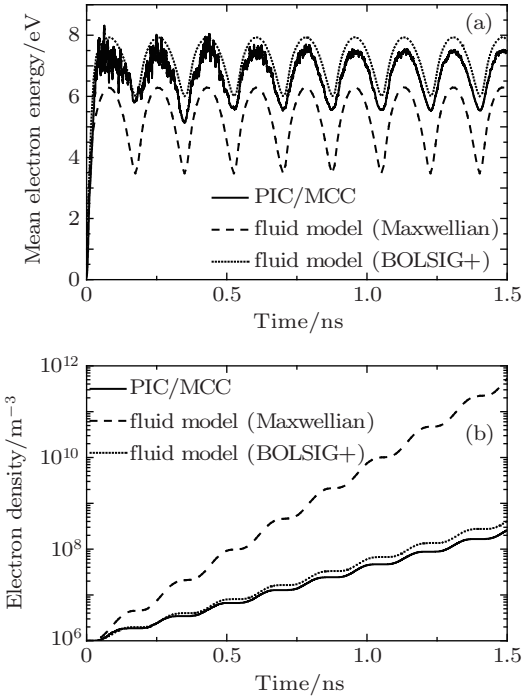


Fig. 3. The time evolution of argon breakdown in PIC/MCC, the fluid model with the Maxwellian EEDF, and the fluid model with BOLSIG+ EEDF: (a) mean electron energy, (b) electron density. Here $p = 500$ Torr, $E_m = 2.82$ MV/m, and $f = 2.85$ GHz.

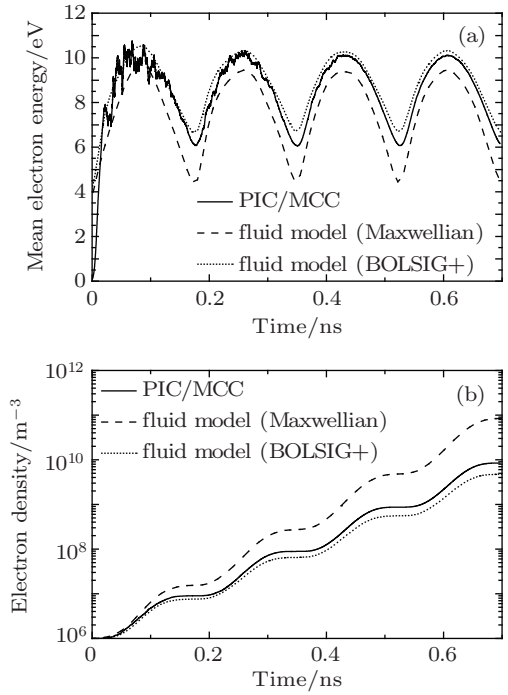


Fig. 4. The time evolution of argon breakdown in PIC/MCC, the fluid model with the Maxwellian EEDF, and the fluid model with BOLSIG+ EEDF: (a) mean electron energy, (b) electron density. Here $p = 200$ Torr, $E_m = 2.82$ MV/m, and $f = 2.85$ GHz.

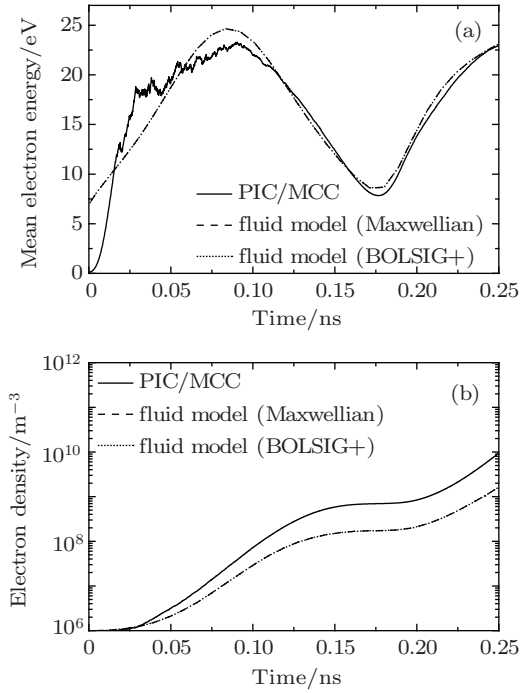


Fig. 5. The time evolution of argon breakdown in PIC/MCC, the fluid model with the Maxwellian EEDF, and the fluid model with BOLSIG+ EEDF: (a) mean electron energy, (b) electron density. Here $p = 50$ Torr, $E_m = 2.82$ MV/m, and $f = 2.85$ GHz.

Figure 6 shows the breakdown time in argon at $E_m = 2.82$ MV/m and $f = 2.85$ GHz over the pressure range 10–1000 Torr. The breakdown time is defined as the time in which the electron density reaches 10^8 times the initial density.[11] The breakdown time of the fluid model with the Maxwellian EEDF reasonably matches that in the PIC/MCC simulations below 100 Torr. However, above 100 Torr, the results with the Maxwellian EEDF become poor. This is because the Maxwellian EEDF produces the overestimated energy tail in non-equilibrium, and leads to the higher ionization frequency, as shown in Figs. 1(a), 1(b), and 2(a). The prediction of the fluid model with the BOLSIG+ EEDF, however, is very well matched to the PIC-MCC prediction over all pressures.

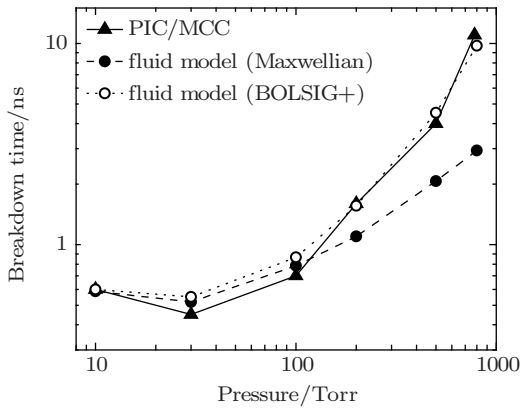


Fig. 6. The breakdown time in argon at $E_m = 2.82$ MV/m and $f = 2.85$ GHz from the PIC/MCC method, the fluid model with the Maxwellian EEDF, and the fluid model with the BOLSIG+ EEDF.

We also confirm that the EEDF in nitrogen predicted

by the BE solver BOLSIG+ approximates well that in the PIC/MCC simulations. As a result, the breakdown time of the fluid model with the BOLSIG+ EEDF agrees well with the PIC/MCC prediction, as shown in Fig. 7. In Fig. 7, the breakdown time in nitrogen at $E_m = 4.0$ MV/m and $f = 2.85$ GHz is shown as a function of the pressure. It can be seen from this figure that the fluid model with the Maxwellian EEDF can predict the breakdown time similar to that of the PIC/MCC simulations. This is because the EEDF in nitrogen breakdown deviates slightly from the equilibrium, as described in Ref. [11].

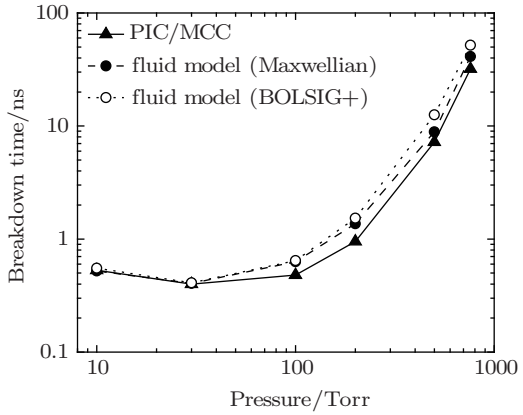


Fig. 7. The breakdown time in nitrogen at $E_m = 4.0$ MV/m and $f = 2.85$ GHz from the PIC/MCC method, the fluid model with the Maxwellian EEDF, and the fluid model with the BOLSIG+ EEDF.

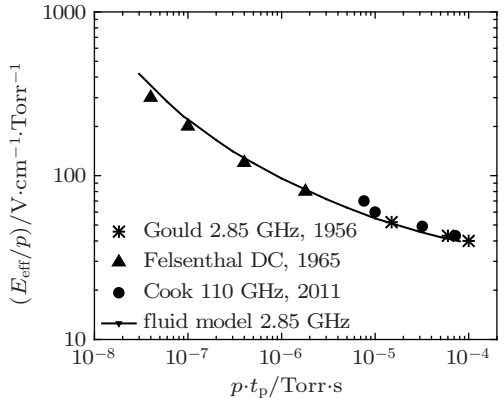


Fig. 8. The comparison between the effective breakdown threshold from the fluid model with the BOLSIG+ EEDF and various experimental results.[20–22]

By using the fluid model with the BOLSIG+ EEDF, the breakdown threshold E_b for air at $f = 2.85$ GHz and $t_p = 30$ ns is predicted over a wide range of pressures. The reason for choosing air is that the corresponding experiments for DC, 2.85 GHz, and 110 GHz are available in the literature.[20–22] In Fig. 8, the effective breakdown threshold ($E_{eff} = E_b/\sqrt{2(1+\omega^2/\nu_c^2)}$) from the fluid model and the experiments normalized to the pressure is shown as a function of pt_p (the pressure times the pulse width). It can be seen that the breakdown prediction from the fluid model with the BOLSIG+ EEDF agrees very well with the experiment results.

4. Conclusion

In this paper, the EEDF from the BE solver BOLSIG+ is introduced into the fluid model, and its validity for studying the argon, nitrogen, and air breakdowns by the HPM is examined by comparing with the results of the PIC/MCC simulations as well as the experimental data. Our results show that the fluid model with the Maxwellian EEDF predicts faster breakdown in argon than the PIC/MCC simulation does at high pressures. This can be explained by the fact that the high-energy tail of the Maxwellian EEDF leads to an overestimation of the ionization frequency. In nitrogen, the EEDF deviates slightly from the equilibrium, so the breakdown time of the fluid model with the Maxwellian EEDF reasonably matches the PIC/MCC prediction. The prediction of the fluid model with the BOLSIG+ EEDF, however, is very well matched with the PIC/MCC prediction in argon and nitrogen. We also confirm that the BOLSIG+ EEDF is valid for the air breakdown based on the experimental results.

References

[1] Li W, Liu Y, Shu T and Qian B 2012 *Chin. Phys. B* **21** 088401
[2] Fang J, Huang H, Zhang Z, Zhang X, Zhang L, Zhang Q, Hao W, Huang W and Jiang W 2011 *Acta Phys. Sin.* **60** 088402 (in Chinese)
[3] Foster J, Edmiston G, Thomas M and Neuber A 2008 *Rev. Sci. Instrum.* **79** 114701
[4] Zhou Q and Dong Z 2013 *Acta Phys. Sin.* **62** 015201 (in Chinese)
[5] Deng Y and Xiao D 2013 *Chin. Phys. B* **22** 035101
[6] Liu X, Song Y and Wang Y 2011 *Chin. Phys. B* **20** 065205
[7] Cai L and Wang J 2011 *Acta Phys. Sin.* **60** 025217 (in Chinese)
[8] Foster J, Krompholz H and Neuber A 2011 *Phys. Plasmas* **18** 013502
[9] Kim J, Kuo P and Kossey P 1995 *J. Plasma Phys.* **53** 253
[10] Zhao P, Liao C and Lin W 2011 *J. Electromagn. Wave. Appl.* **25** 2365
[11] Nam S and Verboncoeur J 2009 *Computer Phys. Commun.* **180** 628
[12] Zhao P, Liao C, Yang D, Zhong X and Lin W 2013 *Acta Phys. Sin.* **62** 055101 (in Chinese)
[13] Hagelaar G and Pitchford L 2005 *Plasma Sources Sci. Technol.* **14** 722
[14] Verboncoeur P, Alves M and Birdsall C 1993 *J. Comput. Phys.* **104** 321
[15] Cai L and Wang J 2009 *Acta Phys. Sin.* **58** 3268 (in Chinese)
[16] Cai L, Wang J, Zhu X, Wang Y, Xuan C and Xia H 2012 *Acta Phys. Sin.* **61** 075101 (in Chinese)
[17] Yee J, Alvarez R, Mayhall D, Byrne D and Degroot J 1986 *Phys. Fluids* **29** 1238
[18] http://jila.colorado.edu/~avp/collision_data/electronneutral/ELECTRON.TXT
[19] Zhao P, Liao C, Lin W, Chang C and Fu H 2011 *Phys. Plasmas* **18** 102111
[20] Gould L and Roberts L W 1956 *J. Appl. Phys.* **27** 1162
[21] Felsenthal P and Proud J 1965 *Phys. Rev.* **139** 1796
[22] Cook A, Hummelt J, Shapiro M and Temkin R J 2011 *Phys. Plasma* **18** 080707